Ecological Modelling 477 (2023) 110274

Contents lists available at ScienceDirect

Ecological Modelling

journal homepage: www.elsevier.com/locate/ecolmodel

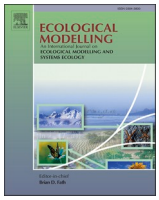

An iterative site-scale approach to calibrate and corroborate successional processes within a forest landscape model

Lucia A. Fitts [a,*], Jacob S. Fraser [b], Brian R. Miranda [c], Grant M. Domke [a,d], Matthew B. Russell [e], Brian R. Sturtevant [c]

[a] Department of Forest Resources, University of Minnesota, 1530 Cleveland Ave. N. St. Paul, MN 55108-6112, United States
[b] USDA Forest Service, Northern Research Station, 202 Natural Resources Building, 1111 Rollins St., Columbia, MO 65211, United States
[c] USDA Forest Service, Northern Research Station, Institute for Applied Ecosystem Studies, 5985 Highway K, Rhinelander, WI 54501, United States
[d] USDA Forest Service, Northern Research Station, 992 Folwell Ave, St Paul, MN 55108, United States
[e] Arbor Custom Analytics LLC, 180 Bangor Mall Blvd #1035, Bangor, ME 04401, United States

ARTICLE INFO

Keywords:
LANDIS-II
Density succession
USDA Forest Inventory and Analysis (FIA) data
Calibration
Equivalence tests
Forest landscape model
Model evaludation

ABSTRACT

Forest landscape simulation models (FLM) have been extensively used for projecting ecosystem dynamics and carbon fluxes. However, more guidance and methods for formal calibration and corroboration of FLMs are needed to ensure higher fidelity results from these models. We developed a novel systematic methodology for calibrating and corroborating a FLM at the grid-cell scale using empirical estimates from the national forest inventory in the United States (US) which uses an equal probability sample design.

We illustrate our approach by using the Forest Inventory and Analysis (FIA) data from the US Department of Agriculture Forest Service across the state of Wisconsin to represent initial site conditions and calibrate parameters for the Density Succession extension of the LANDIS-II model, formally coupled with an iterative model corroboration stage focused on the growth and internal competition component of the model at a site-scale using plot remeasurement data that span 20 years. We used a formal equivalence testing approach to compare model predictions to empirical estimates for permanent sample plots.

We found that the model performed well, with 21 out of 30 species demonstrating equivalence in the estimator used to characterize basal area following initial parameterization. Upon calibration of the estimator, the nine species not initially equivalent all showed reduced bias, with five of the species ultimately passing the equivalence test. The species that did not achieve equivalence through calibration were generally the least abundant ones.

These results have increased our confidence that the Density Succession algorithms were well implemented within the model and provides a useful additional succession option within the LANDIS-II framework. We believe this methodology can capture a wider range of local scale variability compared to previous methods conducted at a landscape level using summary statistics. The iterative nature of the method also gives an opportunity for learning about the model components and the reference plot data. Our approach will help researchers using landscape simulation models to follow a replicable framework for corroborating their results and prioritize forest management activities and land use planning, which can help reduce external pressures on forests and help mitigate climate change effects.

1. Introduction

Forests are ever-changing dynamic biological systems (Peng, 2000). Disturbances play a critical role in forest dynamics (Oliver and Larson, 1996) causing changes in species composition, habitat, and resource allocation. Disturbance regimes are also changing due to global climate change (Seidl et al., 2011, 2017; Turner, 2010; Zhu et al., 2020) and interactions among disturbance types (Sturtevant and Fortin, 2021), threatening habitat conditions in forests and their ability to sustain ecosystem services (Franklin et al., 2007; Seidl et al., 2017). Studies of forest dynamics are key to understanding changes in tree density, species composition, biomass, and carbon sequestration, which are

* Corresponding author.
E-mail address: fitts010@umn.edu (L.A. Fitts).

https://doi.org/10.1016/j.ecolmodel.2023.110274
Received 19 September 2022; Received in revised form 23 December 2022; Accepted 2 January 2023
Available online 11 January 2023

fundamental components of forest ecosystem resilience to climate change.

There are different approaches to studying forest dynamics, one of them being vegetation models which can represent complex, interdisciplinary, and multi-scale spatial processes to address questions about short- and long-term ecosystem dynamics and human-caused or natural drivers of landscape change (Mayer et al., 2016; Mladenoff, 2004). Forest landscape models (FLM) integrate the influence of time and space on environmental drivers and processes that influence vegetation patterns which, in turn, feed back to affect ecological processes (Gao et al., 2018; Peterson, 2002; Shifley et al., 2017).

FLMs have been broadly used especially when long-term forest inventory data are absent to represent forest dynamics in species composition, future yield, succession, disturbances, and ecological restoration purposes, all under diverse environmental conditions (LANDIS II Foundation, 2018; Peng, 2000; Thompson et al., 2016). Over the last three decades, FLMs have increased in detail, complexity and spatial extent with the advancement in technology and computing capacity (Scheller, 2018; Shifley et al., 2017). Despite the power of FLMs to integrate across scales and processes affecting forest dynamics, they are notoriously challenging to validate, impacting confidence in the veracity of their outputs (Scheller, 2018).

Concerns regarding model confidence are not unique to FLMs. There has been an ongoing plea for greater transparency and rigor in the evaluation of ecological and environmental models more generally (Grimm et al., 2010, 2014). Augusiak et al. (2014) coined the term "evaludation" to encompass the full cycle of activities to critically assess whether and when a model is meeting its intended purpose. Two important components of this process are the calibration of model parameters and the corroboration of model outputs.

Calibration, a component of model output verification, is an iterative process of modifying the model parameters one at a time until there is an incremental improvement of the results in comparison to empirical data (Wang et al., 2014). A common method of calibrating species-level parameters within an FLM is to fit model outputs to established empirical estimates of growth and yield (Lucash et al., 2017; Reese et al., 2022). These estimates are often based on averages of observations aggregated over space and time. Model corroboration involves comparing an independent data set with the model predictions from the same temporal and spatial scales within its relevant domain to examine agreement between modeled and empirical data (Augusiak et al., 2014; Shifley et al., 2017). Previous corroboration work has been done for FLMs such as LANDCLIM (Schumacher et al., 2004), iLand (Seidl et al., 2012), and LANDIS PRO (Wang et al., 2014) using aggregated plot data for a short-term (two or three decades). A more novel approach to both calibration and model corroboration is to match model outputs with the behavior of individual plots (i.e., disaggregated). This method has been widely applied to plot scale models (Bagdon et al., 2021; Vacchiano et al., 2014), but not yet applied to FLMs.

While similar studies have been conducted within the LANDIS-II model framework (e.g., Boulanger et al., 2017; McKenzie et al., 2019), its distributed development strategy and design has impeded the adoption of a more universal corroboration methodology. To help address this problem, we developed a systematic and disaggregated methodology for calibrating and corroborating a FLM using a pairwise comparison to existing forest inventory data. Our specific research objectives are to (1) build a replicable methodology for model evaluation that can segregate specific areas of the model to evaluate, and (2) increase confidence in model processes by testing the performance of individual model components at the site-level. We believe this methodology can capture a wider range of local scale variability compared to previous methods conducted at a landscape level that use summary statistics. To achieve these objectives, we used estimates from the Forest Inventory and Analysis (FIA) program of the United States Forest Service (USFS) across the state of Wisconsin to represent initial site conditions and calibrate a new succession extension for LANDIS-II (Scheller et al., 2007) - Density Succession - that encapsulates the logic of vegetation dynamics from LANDIS PRO (Wang et al., 2013) into the LANDIS-II model framework. Our approach applies an iterative methodology to progress from calibration to model corroboration stage, illustrated by the growth and internal competition components of the Density Succession extension using 20 years of the FIA plot remeasurement data.

2. Methods

To demonstrate our methodology, we selected a multi-remeasurement inventory dataset (Wisconsin's FIA data) and a FLM (LANDIS-II), where observations from the inventory plots were represented as individual cells (12.97 × 12.97 m) within the FLM. We subdivided our dataset into three groups, each of which were used in different phases of the analysis. We performed an initial fit of model parameters on the first subset group and used the second subset group to test equivalency. We then performed an iterative parameter calibration process using subset groups one and two together. Finally, we simulated subset group 3 using calibrated parameters and tested the model equivalency (See section Simulations for further details). For calibration and corroboration steps, we conducted a pairwise comparison at a cell/plot level.

2.1. The LANDIS-II model

The LANDIS-II FLM combines ecological principles such as succession, disturbance, and ecosystem ecology to represent the changes that occur in vegetation and ecosystem properties and rates, describing both the behavior and state of the system itself (Scheller et al., 2007). The model accounts for interactions among succession, natural disturbances, and management actions at a species level (Mladenoff and He, 1999; Scheller and Mladenoff, 2004), and is spatially dynamic (He, 2008). LANDIS-II is driven by tree species life history attributes, which regulate the way species grow and are distributed across the landscape, as well as species' responses to disturbances. Due to its broad scale of landscape application, the LANDIS-II model does not represent individual trees, but uses collections of tree species-age cohorts, where each cohort carries attributes of age and species (Scheller et al., 2007). The LANDIS-II landscape is represented in a raster format, with individual sites (cells) as the basic spatial unit of the landscape containing tree cohort data, and regions, which are collections of sites that have similar characteristics (e.g., soils, climate, disturbance regime) as a secondary spatial unit.

LANDIS-II is not a single model, but a model framework that consists of a central core that coordinates the plug-in extensions that actually contain the science, with designated extensions that represent the modeled processes of succession, disturbance and model output. For the purposes of this study, we utilized the newly developed Density Succession extension (Fraser et al., 2020) for succession processes, and the Land Use Plus (LU+) extension (Thompson et al., 2016) for disturbances.

2.1.1. Density succession

Density Succession is an extension that ports the forest stand dynamics processes developed for LANDIS PRO (Wang et al., 2013) into the LANDIS-II model framework (Fig. 1). Species within the model are assigned key life history attributes that are common across all LANDIS-II succession extensions including longevity, shade tolerance, age of sexual maturity, minimum age for sprouting (and its probability), seeding distance, and fire tolerance. Additionally, Density Succession tracks the number of trees and diameter by species-age cohort on each active site (Fraser et al., 2020), which is also how LANDIS PRO operates (Wang et al., 2013). The succession, competition, and establishment processes use additional species- and site-level parameters to estimate the occupied proportion of available growing space (Fraser et al., 2020; Wang et al., 2013). Estimates of stand density, basal area, stocking, and

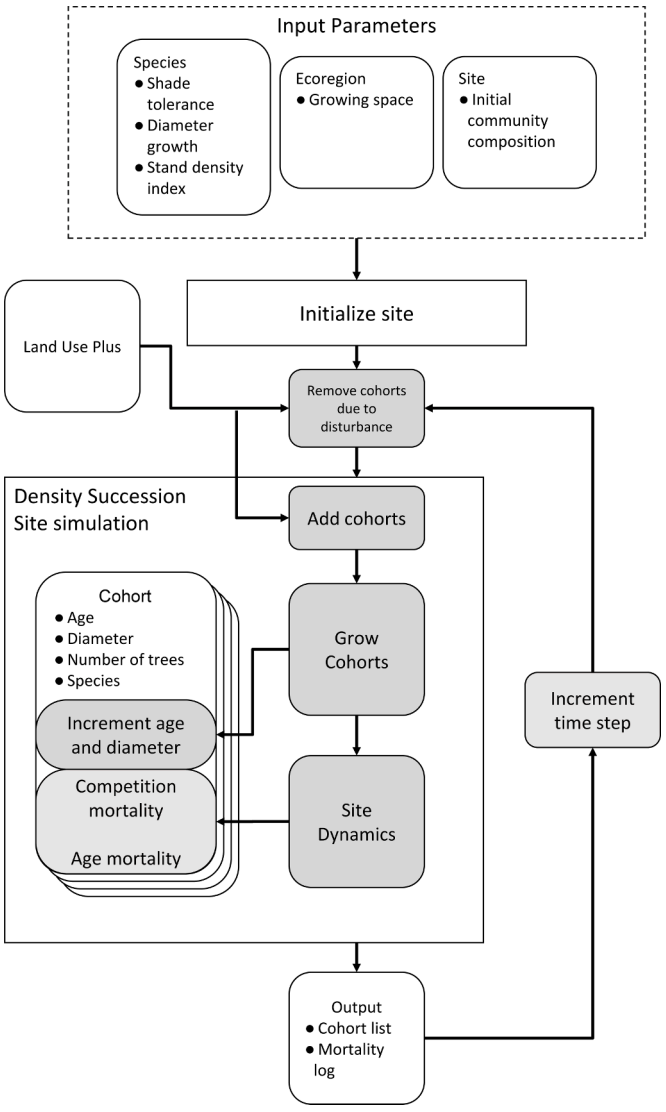

Fig. 1. Conceptual diagram detailing the sequence of model operations for the Density Succession and Land Use Plus extensions of LANDIS-II.

biomass (through allometric equations) can be derived from the number of trees and diameter for each cohort.

Site-level resource competition is modeled using a stand density index (*SDI*) to quantify growing space occupied (*GSO*) and maximum growing space (*MGS*) (Reineke, 1933; Woodall et al., 2005). SDI_{ij} is calculated for each cohort present on a site with a reference diameter of 25.4 cm, using Eq. (1), where NT_{ij} is the number of trees and DBH_{ij} is the diameter in cm of cohort *j* in species *i*. The SDI parameter is defined in units of number of reference trees per hectare, therefore the minimum growing space ($MinGS_i$) for a single reference tree of 25.4 cm for each species is calculated using the inverse of the maximum SDI parameter ($MaxSDI_i$) defined per species (Eq. (2)). The *GSO* for a given site is calculated using Eq. (3) as the sum SDI_{ij} times $MinGS_{i\_standard}$ transformed to be relative to the area of sites within the model.

$$SDI_{ij} = \left(\frac{DBH_{ij}}{25.4}\right)^{1.605} \times NT_{ij} \tag{1}$$

$$MinGS_i = \frac{10000}{MaxSDI_i} \tag{2}$$

$$GSO = \sum_{i=1}^{No.\ Species} \sum_{j=1}^{No.\ Cohorts} SDI_{ij} \times \frac{MinGS_i}{site\ area} \tag{3}$$

If the site-level *GSO* value exceeds the ecoregion-level parameter for *MGS* then Density Succession implements self-thinning through a modified version of an SDI-based mortality model (Crookston and Dixon, 2005; Dixon, 1986; Johnson and Dixon, 1986). The probability of mortality ($PMORT_{ij}$, Eq. (4)) is calculated for each cohort using the cohort's diameter relative ($RELDIA_{ij}$, Eq. (5)) to the site's quadratic mean diameter (QMD_{site}), and a shade tolerance weighting factor (SWF_i) determined by the species-level shade tolerance parameter (Dixon, 2002; Stage, 1973). Species have a defined shade tolerance value ranging from one to five with one being the most shade intolerant and five being the most shade tolerant.

$$PMORT_{ij} = \left(0.84525 - \left(0.01074 \times RELDIA_{ij}\right) + \left(0.0000002 \times RELDIA_{ij}^3\right)\right) \times \left(1 - SWF_i\right) \tag{4}$$

$$RELDIA_{ij} = \frac{DBH_{ij}}{QMD_{site}} \tag{5}$$

Once the probability of mortality has been calculated for all cohorts on the site, they are sorted in descending order and a function loops through checking the value of $PMORT_{ij}$ against a uniform random distribution. If the uniform random distribution draw is less than $PMORT_{ij}$, then a single stem is removed from the cohort and the calculated growing space of the stem is subtracted from *GSO*. This loop continues through all cohorts and makes multiple passes through the list, if necessary, until *GSO* is less than the *MGS* ecoregion parameter.

2.1.2. Land use plus

The Land Use Plus (LU+) extension is a disturbance extension within LANDIS-II that incorporates land use, land cover change, and other disturbances into the simulation. Despite the extension's name, LU+ allows the user to do more than just represent land use change. It integrates specific predefined (spatially and temporally explicit) disturbance events that could be externally developed, empirical observations, specific prescriptions (e.g., plantations, harvests), or specific spatio-temporal processes (e.g., land use or disturbance representations) into LANDIS-II simulations (Thompson et al., 2016; J. 2021). LU+ uses categorical or thematic raster maps for each time step representing the different change or disturbance processes to be simulated. Changes indicated by the map series are incorporated into the simulations as disturbances to the cohorts on impacted sites. Users specify the impact to species age cohorts, including the amount of biomass to be removed, new cohorts added through planting, as well as the option to prevent establishment following the change (Thompson et al., 2016).

2.2. The forest inventory and analysis data

For this study, we used subsets of the Forest Inventory and Analysis (FIA) dataset to represent initial site conditions, calibrate model parameters, and test for equivalency. We used Wisconsin's plot data collected by the FIA program from 2000 (the start of Wisconsin's annual inventory) until 2020 (Burrill et al., 2018).

The FIA program focuses on monitoring forestland conditions in the US across all ownerships. As with other states in the eastern continental US, each of Wisconsin's FIA plots with at least one forested condition (i.e., a mapped domain on FIA plots) is remeasured approximately every five years with attention to the growth and mortality of previously recorded trees as well the ingrowth of new trees. The FIA program uses an equal probability sampling design where all elements of the population have the same probability of being sampled by a ground plot (Bechtold and Patterson, 2005). The design-based estimators used to

obtain estimates from the FIA program can be assumed to be unbiased for large samples (Stanke et al., 2022). The sample area covered by each FIA plot is 0.4 hectares, divided into four fixed-radius (7.32 m) permanent sample subplots. Trees with a diameter at breast height (dbh) greater than or equal to 12.7 cm are recorded in each subplot. These four subplots are distributed with subplot one being at the center and subplots two, three, and four are located 36.6 m away at azimuths of 120°, 240°, and 360° respectively. Within each subplot, a microplot of 2.07 m radius is nested, where trees with a dbh between 2.54 cm and 12.7 cm are recorded. For our approach, we used the four subplots that make up a plot for different stages of our analysis. We used one subplot for the initial fit of model parameters, a second subplot was used for testing equivalency, and the two remaining subplots were combined to represent our third group for our second corroboration round. Subplots from each plot were randomly assigned to these groups.

Within each subplot, FIA records certain information at a condition-level. A condition is defined by changes in land use or vegetation that occur inside a plot. Each forested condition is mapped according to reserved status, owner group, forest type, stand density, etc. (Burrill et al., 2018).

We used data from trees greater or equal to 2.54 cm dbh to initialize our sites in the LANDIS-II model, to calibrate model parameters, and to corroborate the Density Succession extension growth algorithms. The trees recorded in the microplots (< 12.7 cm dbh) represent regeneration ("ingrowth") in the FIA database and were used in our analysis to represent establishment of new tree species cohorts (See Land Use Plus section) utilizing the microplot expansion factor (TPA_UNADJ, Burrill et al., 2018). This expansion factor represents the number of trees per acre that are theoretically represented by the sample tree based on the FIA sample design (Burrill et al., 2018). The use of this expansion factor allowed us to scale inventory tree regeneration records to match the area simulated in each site. For this research, due to the scale, desired level of detail, and the ability for Density Succession to reduce density to reflect individual tree deaths, we used the agent code as the cause of mortality. This variable is useful when information about disturbances that affect individual trees is desired (Fitts et al., 2022).

2.3. General considerations

Our approach is based on a cell-level assessment, with each cell representing a single FIA subplot. Therefore, we used a cell size of 12.97 × 12.97 m, which corresponds to the area of a FIA subplot (168.33 m^2). For computing efficiency, all the FIA subplots (cells) available for Wisconsin were run independently but configured in a single simulation landscape without interaction between cells - where natural regeneration (e.g., seeding) was prevented and disturbances were applied individually at the cell scale (Fig. 1). Each subplot was assumed to be homogeneous with respect to forest type and age distribution, consistent with LANDIS-II assumptions.

2.4. Data preparation

The pool of simulated plots is composed of FIA plots in the state of Wisconsin filtered to plots classified with a forested land cover at the start of the study period (2000). These plots consisted of either forested or mixed conditions (partial forest/non-forest plot, e.g., one forest plus one non-forest condition) that had trees present at the initial time step. We further refined our selection to include only plots that had remeasurements available for at least 3 points in time (*t0, t1,* and *t2*), making a total of 4895 plots that were used. Wisconsin has data from four FIA remeasurements (each time a plot is re-evaluated by the field crew) which allows for a robust spatiotemporal analysis.

Between 2000 and 2020, 95.3% of the subplots consisted of a single condition, while almost 4.7% had two conditions present. The high number of subplots that had only one condition reinforced our decision to work at the subplot level to achieve homogeneous units. For each FIA plot we randomly assigned subplots to three groups (hereafter A, B, and C), with a single subplot in groups A and B, and the remaining two assigned to group C. Each subplot group (or combination of them) was used for different purposes described in the calibration and corroboration sections (Fig. 2). This approach ensures representation of each plot but with a direct translation between inventory data into LANDIS-II's cells without further aggregation.

There were 92 species present in Wisconsin's FIA subplots. The three most abundant hardwood species were red maple (*Acer rubrum*), quaking aspen (*Populus tremuloides*), and sugar maple (*Acer saccharum*). The three most abundant conifer species were red pine (*Pinus resinosa*), balsam fir (*Abies balsamea*), and northern white cedar (*Thuja occidentalis*). Since less than a third of the species represented 99% of the total number of trees, we selected the 30 most abundant (Verberk, 2012) species in the ecosystem and created an additional six generic categories to represent life history attributes for those remaining (Table 1). The categories created were large shade tolerant hardwood (L-T-H), large shade tolerant conifer (L-T-C), large shade intolerant hardwood (L-I-H), large shade intolerant conifer (L-I-C), small-medium shade tolerant hardwood (S-T-H), and small-medium shade intolerant hardwood (S-I-H). No small sized conifers were present in the data set, so no generic categories were created for small conifers. Some of the less frequent species were crosswalked to another species that had similar life history attributes (i.e., longevity, sexual maturity, shade tolerance, and fire tolerance) within our selected 30 species (See Table S-1 for a complete list of species present in our dataset and the re-categorization performed on the least abundant species (<%1 of the trees)). We reclassified the remaining low abundance species into the six generic categories according to their life history attributes. From these, there were 16 species categorized as small-medium tolerant hardwoods, nine species categorized as small-medium intolerant hardwoods, two species categorized as large tolerant hardwoods, two as large tolerant conifers, three categorized as large intolerant hardwoods, and one large intolerant conifer.

There are 40 ecological subsection codes in Wisconsin (ECOSUBCD, Burrill et al., 2018; McNab et al., 2007), 12 ecological sections, and two provinces (Laurentian Mixed Forest Province and Midwest Broadleaf Forest Province). We selected the ecological sections to represent ecoregions in our simulations to balance representation of major differences in productivity across the state with the need for adequate plot sample sizes in each ecoregion. We used the ecological sections attribute to characterize each subplot's growing environment. Diameter growth models for each species in each ecological section were estimated with the *vitalRates* function in the rFIA package for trees larger than 12.7 cm dbh (Stanke et al., 2020). For trees less than 12.7 cm dbh we calculated average annual diameter growth from remeasurement records in FIA for each species in each ecological section.

Disturbances (including the year when they occurred) were processed from the agent of mortality (AGENTCD) variable in FIA (Burrill et al., 2018). This variable records the cause of death (agent) of a tree which was alive at the previous measurement and is now dead or removed. The "*vegetation*" agent of mortality code was removed from the disturbances since self-thinning is already incorporated into Density Succession (the model should remove these trees via internal self-thinning routines) and was one of our evaluation variables. The "*other*" mortality code was also removed from the disturbances since the reason for mortality was not clearly identified and we assumed this was either part of the competition mortality or it would be accounted for by the incorporated background mortality in the model. Both self-thinning and background mortality are stochastic processes within the Density Succession extension.

Model parameters for each species were defined using information from previous studies, available literature, and expert knowledge (Table 1). Maximum stand density index values (maxSDI) were obtained from USDA Forest Service (2019). Species life history attributes (e.g., longevity, shade tolerance) were also obtained from the literature.

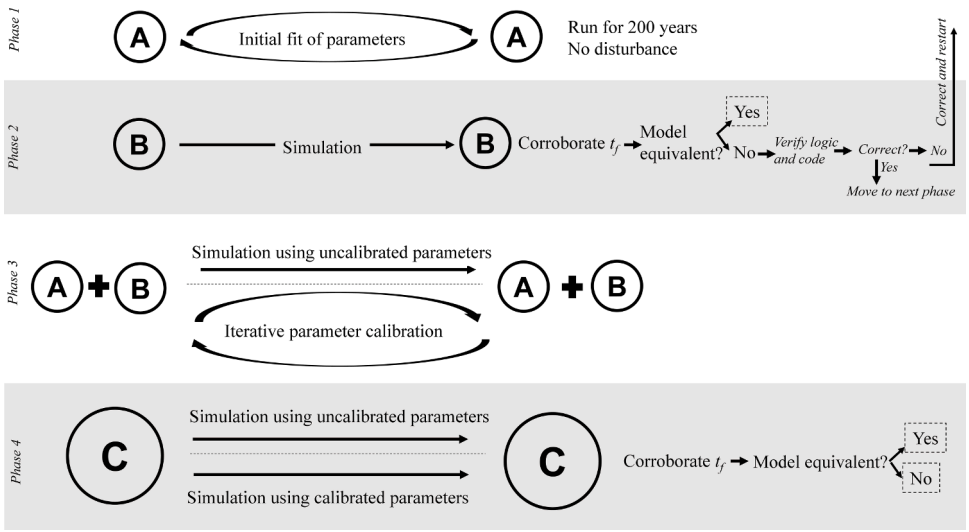

Fig. 2. Visual representation of the different phases of corroboration and calibration processes. Each letter represents a set of subplots selected for different stages in the process. For each FIA plot, the position of the letters was randomly assigned, with two of the nested subplots assigned to group C (A and B, $n = 4895$; C: $n = 9790$). *Tf* indicates the final time step for that simulation.

Species attributes for the generic categories were assigned values from representative species. ForL-I-H we used the value for quaking aspen (*Populus tremuloides*), for L-T-H we used sugar maple (*Acer saccharum*), for S-T-H we used eastern hophornbeam (*Ostrya virginiana*), for S-I-H we used hawthorn (*Crataegus* spp.), for L-I-C we used red pine (*Pinus resinosa*), and for L-T-C we used balsam fir (*Abies balsamea*). See Methods-Simulations for a list of the parameters set to zero.

2.5. Simulations

LANDIS-II requires several text and raster map files to provide model inputs. The main file is the scenario text file, which contains the specific instructions and details for the simulation. See the Density Succession user guide (Fraser et al., 2020) for a complete list of input files needed for the succession extension. We ran different sets of simulations using LANDIS-II starting at time zero (t_0) for 20 years. We set the model so the succession process would occur at a one-year time-step due to possible inconsistent remeasurement intervals where disturbances and establishment are recorded. This approach allowed us to intervene in the timeline when an event (disturbance or establishment) happened in specific cells but make no change to the cells where no events happened.

Seed dispersal was set to one while reproduction probability, sprouting, and post-fire regeneration were set to zero to prevent cell interaction and to control the disturbances and establishment occurring in the simulated subplot. The species values of fire tolerance and sexual maturity age were ignored by the model due to the decision to disable disturbance events and seed production. Longevity was given an arbitrary number of 400 for all species.

This approach allowed us to isolate our evaluation and corroboration to focus on the growth and competition behaviors of the model. We used a modified version of LU+ to remove individual stems when documented disturbances happened and to plant new stems recruited to the minimum diameter class recorded in the FIA data. We did not add trees that were recruited at the subplot level (greater or equal to 12.7 cm dbh) in future remeasurements, only those recruited at the microplot level. This was done to prevent repetition of stems since the microplot was scaled up to the subplot level (with the FIA expansion factor [TPA_UNADJ]) and was assumed to be representative of the subplot in density and species.

The process of the simulations that included calibration and corroboration phases occurred in an iterative and stepwise way, with different groups of subplots reserved for each stage in the process (Fig. 2).

2.5.1. Phase 1: initial parameter fit

Subplots randomly assigned to group A were used to fit one initial model parameter (maximum growing space *MGS,* See Methods-Density Succession section) at an ecoregion-level. Calibrating *MGS* for each ecological section required fitting a model of maximum basal area to different levels of *MGS* values. On this set of simulations, *MGS* was adjusted upward by 0.1 increments starting with a value of 1.0 up to and including the value of 2.0. The simulations were run for 200 years with no disturbance (LU+ was turned off for these runs), which allowed the plots to grow to peak basal area and let the model's self-thinning algorithms control the dynamics. After we ran the simulations with the varying *MGS* values, we created a linear regression model in R between *MGS* as the response variable and maximum basal area (95 percentile) as the predictor variable. In parallel, we used the rFIA package (Stanke et al., 2020) to obtain the maximum basal area total stocking for all the forested plots within the Wisconsin's FIA database (ALSTKCD variable). We fit a quantile regression model using the 95th percentile of basal area predicted by total stocking for each ecological section. A prediction of basal area from the quantile regression model for a stocking value of 100% was generated for each ecological section and used in the corresponding linear regression model to predict a value for *MGS* for each ecoregion. The *MGS* value obtained for each ecoregion was used for the remaining phases of the analysis.

2.5.2. Phase 2: model corroboration

After estimating *MGS*, we used the B subset of subplots for the second model run, with which we corroborated the model outputs against observed tree density, mean tree diameter, and basal area. During this corroboration, we determined regions of agreement and regions of discrepancy. At this stage we verified that the observed inventory data was correctly represented within the model and that the assumptions of ingrowth establishment and non-competition mortality were enacted properly (Fig. 2). In addition, we verified the computer code (for both the model itself and for data analysis) by checking for errors, bugs and oversights, as well as confirming the model was performing according to design (*implementation verification*, Augusiak et al., 2014).

Corroboration allowed us to compare the simulated and observed outputs and evaluate the model performance. The site scale corroboration was done through comparing raster cell-level predictions with inventory data to explore individual cell deviation from the corresponding

Table 1
Species life history traits and abundance for species present in Wisconsin's inventory data at time 0.

Common name	Scientific name	Shade tolerance[1,2]	Max SDI[3]	N trees ≥12.7 cm sampled	N plots that contained the species	Cumulative percentage (number of trees)
red maple	*Acer rubrum*	3	421	15,533	5108	11.74
quaking aspen	*Populus tremuloides*	1	562	14,204	3833	22.47
sugar maple	*Acer saccharum*	5	371	13,829	3872	32.92
red pine	*Pinus resinosa*	2	505	7482	1197	38.57
northern white-cedar	*Thuja occidentalis*	4	771	6682	1002	43.62
paper birch	*Betula papyrifera*	2	466	6352	2497	48.42
balsam fir	*Abies balsamea*	5	655	6134	2211	53.05
northern red oak	*Quercus rubra*	2	414	5513	2221	57.22
American basswood	*Tilia americana*	4	526	5072	2023	61.05
black ash	*Fraxinus nigra*	4	423	4872	1424	64.73
American elm	*Ulmus americana*	3	282	4337	2076	68.01
eastern white pine	*Pinus strobus*	3	529	3789	1380	70.87
jack pine	*Pinus banksiana*	1	356	3660	861	73.63
bigtooth aspen	*Populus grandidentata*	1	520	3446	1085	76.24
white oak	*Quercus alba*	3	361	3052	1455	78.54
northern pin oak	*Quercus ellipsoidalis*	2	336	2782	898	80.65
tamarack (native)	*Larix laricina*	1	387	2704	695	82.69
black oak	*Quercus velutina*	2	370	2550	813	84.61
black spruce	*Picea mariana*	3	500	2443	664	86.46
yellow birch	*Betula alleghaniensis*	3	369	2295	1217	88.19
black cherry	*Prunus serotina*	3	384	2135	1289	89.81
eastern hemlock	*Tsuga canadensis*	5	510	1953	711	91.28
green ash	*Fraxinus pennsylvanica*	3	414	1763	730	92.62
white ash	*Fraxinus americana*	4	408	1725	924	93.92
white spruce	*Picea glauca*	4	412	1504	618	95.06
bur oak	*Quercus macrocarpa*	2	423	1305	631	96.04
bitternut hickory	*Carya cordiformis*	2	301	1277	683	97.01
shagbark hickory	*Carya ovata*	3	302	965	474	97.73
eastern hophornbeam	*Ostrya virginiana*	4	304	939	595	98.44
boxelder	*Acer negundo*	3	344	923	389	99.14
L-I-H	Large intolerant hardwood	1	562	302	80	99.37
L-I-C	Large intolerant conifer	2	505	274	113	99.58
S-I-H	Small intolerant hardwood	2	463	245	138	99.76
L-T-H	Large tolerant hardwood	5	371	228	143	99.93
S-T-H	Small tolerant hardwood	4	257	86	59	100.00
L-T-C	Large tolerant conifer	4	655	1	1	100.00

[1]Lucash et al., 2017.
[2]Burns & Honkala (1990).
[3]FVS Staff (2021).

FIA data. The model outputs were corroborated using the data from the last FIA remeasurement (t_f). During phase 2, the output variables used for corroboration were total basal area (m^2/ha), density (number of trees), and mean diameter (cm) per ecoregion and per species. Each observation point was a subplot.

To verify if there were significant differences between simulated and observed estimates for each corroboration variable, equivalence tests were performed (Lakens, 2017; Robinson and Froese, 2004). Equivalence tests permit a dissimilarity based on a specified threshold that allows some amount of disagreement between observed and predicted values (Lakens et al., 2018). The benefit of this approach is that we put the burden of proof on the alternative hypothesis, which in this application was that both LANDIS-II and FIA outputs (means of the response variables) are equivalent. The validity of the model is then assessed by examining the accuracy of model predictions. The TOST procedure consists of Two One-Sided T-tests. The first one-sided test is used to test the estimate against values at least as extreme as the lower equivalence bound (ΔL) and the second one-sided test is used to test the estimate against values at least as extreme as the upper equivalence bound (ΔU). Both of these one-sided t-tests need to be significant for equivalence to be assumed (See Lakens et al., 2018 for a complete description of equivalence tests). The TOST variables were the mean of the differences between simulated (s, the LANDIS-II output) and observed (o, the FIA empirical data) values for total basal area, density, and mean diameter per species and per ecoregion. The null hypothesis is that the means are different (H0: $\mu_s - \mu_o \neq 0$, dissimilarity), and the alternative hypothesis is that the means are the same.

We used the *TOSTER* R package (Lakens, 2017) to perform two one-sided t-tests of equivalence (TOST) with an alpha of 0.05 and epsilon values of 0.5 (Blanco et al., 2007; Robinson and Froese, 2004). We had paired data between FIA observations and LANDIS-II projections, and therefore used the *dataTOSTpaired()* R function (Lakens, 2017). We performed three equivalence tests at phase 2 of the simulations: total basal area per species (1), mean diameter per species (2), and density per species (3).

The first round of corroboration with the B subplots, was followed by a model calibration phase (Phase 3). Upon completion of calibration, a second round of corroboration was done using the same equivalence testing methods with the C subplot group, maintaining consistent sample sizes between calibration and corroboration, where we again determined regions of agreement and regions of discrepancy (Phase 4).

2.5.3. Phase 3: parameter calibration

After initial corroboration, we performed a stepwise calibration

using the combined A and B groups of subplots (Fig. 2). The goal of the calibration was to minimize discrepancies and retain agreements identified in the initial corroboration. Because the density variable performed well during phase 2, the calibration phase focused on adjusting the mean diameter and total basal area to match observed FIA data. To achieve this, we adjusted the age-diameter curves, which control the growth rates for each species in every ecoregion and directly affect mean diameter and total basal area (our variables of interest). Only species that failed the second round of corroboration equivalence test for basal area (9 species when using the combined A and B groups) were targeted for parameter adjustment. For each species undergoing calibration, we applied proportional adjustment factors ranging between 0.05 and 3.0, in increments of 0.05, to increase or decrease growth at a specific ecological section of the growth curve as needed. This over or under estimation of growth was evaluated with scatterplots of observed vs predicted values (Fig. 3) for mean diameter. The scatterplots were used to identify which diameter growth model (<12.7 cm dbh, ≥12.7 cm dbh, or both) would need adjustments. This threshold is the one that separates the trees measured in the FIA program at a microplot from a subplot level.

To achieve calibration, we created R code that interacts with the input files of each extension until an optimal adjustment factor (minimized residual bias) for each parameter was reached. We chose adjustment factors that minimized mean bias for basal area when doing equivalence tests with an epsilon of 0.5. These values were carried to the next phase. In addition, we ran a simulation using the same A and B group subplots with non-calibrated parameters to ensure that the differences observed from the previous phase (Phase 2 Corroboration) were actually due to calibrated parameters and not due to an increase in sample size.

2.5.4. *Phase 4: final model corroboration*

In this phase, we conducted the TOST equivalence tests using group C (Fig. 2) with an epsilon of 0.5 and the same hypothesis described in

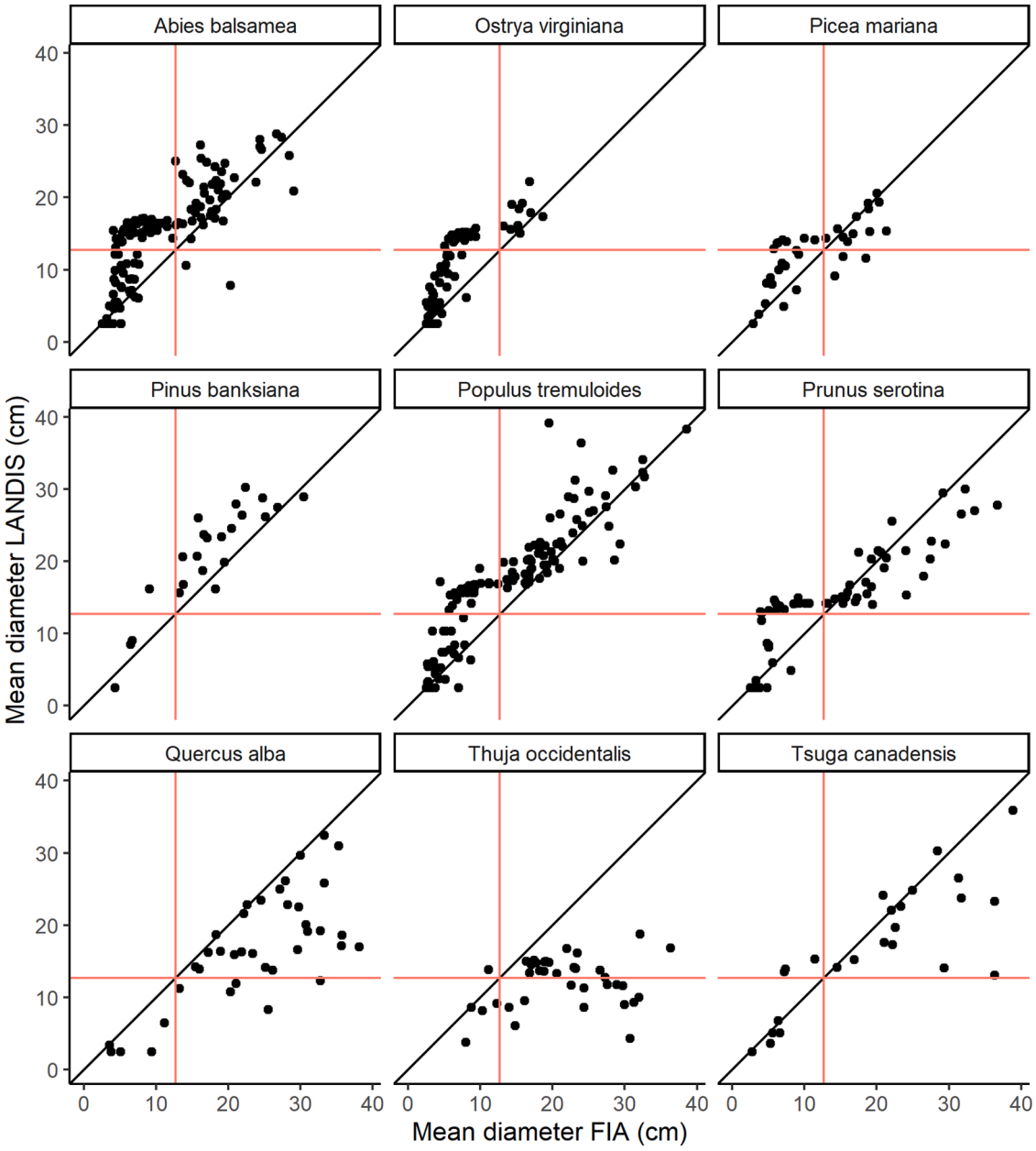

Fig. 3. Observed vs predicted values for the mean diameter variable (cm) for the nine species that failed the initial corroboration equivalence tests. The red perpendicular lines mark the 12.7 cm threshold that separates the trees measured in an FIA subplot vs a microplot.

section Phase 2: Corroboration. We performed two TOST tests in parallel, one using non-calibrated parameters and the other using the calibrated parameters (Table 4). This was done to see if the difference that occurred in the results was actually due to the calibrated parameters instead of due to the use of a different sample.

3. Results

3.1. Phase 1: initial fit of maximum growing space parameter

Observed 95th percentile basal areas across all ecological sections ranged from 39 to 52 m^2/ha and the calibrated values for *MGS* ranged from 0.93 to 1.69 (Table 2). See supplementary figure S-2 for visual outputs of the different runs for subplot group A.

3.2. Phase 2: model corroboration

We observed that density outputs from LANDIS-II simulations were equivalent for 29 out of the 30 most abundant species (Table 3). For mean diameter, 22 out of the 30 most abundant species fell into the equivalence range. LANDIS-II simulations under-predicted the mean diameter for *Abies balsamea, Ostrya virginiana, Pinus banksiana*, and *Populus tremuloides* and over-predicted for *Quercus alba, Thuja occidentalis, Tilia americana*, and *Tsuga canadensis*. For basal area, 20 out of the 30 most abundant species were equivalent with an epsilon of 0.5. LANDIS-II simulations tended to under-estimate basal area. The species that fell into this category were *Abies balsamea, Ostrya virginiana, Picea mariana, Pinus banksiana, Populus tremuloides*, and *Prunus serotina*. The species whose output was over-estimated were *Pinus resinosa, Quercus alba, Thuja occidentalis*, and *Tsuga canadensis*.

3.3. Phase 3: parameter calibration

From the observed vs predicted scatterplots (subplots $A + B$) for mean diameter (Fig. 3), we noticed that the diameter growth models for *Abies balsamea, Ostrya virginiana*, and *Prunus serotina* were over-predicting the diameter for trees <12.7 cm dbh. The models for *Pinus banksiana* were overpredicted for trees larger or equal than 12.7 cm dbh. *Picea mariana* and *Populus tremuloides* were overpredicted across the entire dbh range. The mean diameter was underpredicted for *Tsuga canadensis* under 12.7 cm dbh and for *Quercus alba* and *Thuja occidentalis* across the entire diameter range.

After iterative adjustments, all nine calibrated species showed equivalence (Table 4). The proportional adjustment selected to apply for the next corroboration phase was the one for each species that made the

Table 2
Estimated maximum growing space and basal area reached per ecological section in Wisconsin, USA.

Ecological section code	Ecological section name	Number of plots	Maximum basal area (m^2/ha)	Maximum growing space
212J	Southern Superior Uplands	174	49.13	1.29
212K	Western Superior Uplands	384	39.06	1.05
212Q	North Central Wisconsin Uplands	393	44.15	1.39
212T	Northern Green Bay Lobe	569	52.17	1.48
212X	Northern Highlands	1605	43.84	1.52
212Y	Southwest Lake Superior Clay Plain	173	45.16	1.06
212Z	Green Bay-Manitowoc Upland	87	49.19	1.43
222K	Southwestern Great Lakes Morainal	352	44.85	1.09
222L	North Central U.S. Driftless and Escarpment	767	44.7	1.69
222M	Northern Minnesota and Ontario	40	42.63	0.93
222R	Wisconsin Central Sands	351	42.72	1.22

Table 3
Results from the simulations with group B subplots for density (trees/ha), mean diameter (cm) and basal area (m^2/ha). Cells in bold and with the † symbol represent an equivalent result for the equivalence tests (TOST) with an epsilon of 0.5. Mean bias in the estimator used to obtain predictions is calculated as the difference between observations and predictions.

Scientific name	N	Density	Mean diameter	Basal area
		Mean bias (SD)	Mean bias (SD)	Mean bias (SD)
Abies balsamea	562	**-1.08 (16.59)**†	3.94 (4.07)	0.19 (0.21)
Acer negundo	84	**1.83 (9.91)**†	**-1.45 (8.46)**†	**0.05 (0.16)**†
Acer rubrum	1003	**-2.88 (11.82)**†	**-0.23 (6.73)**†	**0.00 (0.13)**†
Acer saccharum	905	**0.94 (7.55)**†	**-2.94 (8.10)**†	**-0.02 (0.15)**†
Betula alleghaniensis	158	**-1.92 (10.41)**†	**-2.92 (8.82)**†	**-0.02 (0.09)**†
Betula papyrifera	201	**-0.58 (9.57)**†	**0.63 (5.29)**†	**0.04 (0.11)**†
Carya cordiformis	94	**-0.43 (4.97)**†	**-1.28 (7.74)**†	**0.00 (0.10)**†
Carya ovata	73	**-0.36 (5.27)**†	**-1.07 (7.06)**†	**0.01 (0.09)**†
Fraxinus americana	192	**-0.88 (8.44)**†	**0.22 (6.41)**†	**0.04 (0.12)**†
Fraxinus nigra	324	**-2.81 (12.07)**†	**-0.38 (5.61)**†	**0.00 (0.12)**†
Fraxinus pennsylvanica	131	**-0.60 (6.37)**†	**0.38 (5.35)**†	**0.01 (0.13)**†
Large intolerant conifer	15	-4.53 (13.63)	1.73 (2.68)	0.01 (0.07)
Large intolerant hardwood	9	0.11 (4.17)	1.24 (2.14)	0.01 (0.10)
Large tolerant hardwood	49	**-0.37 (3.87)**†	-4.60 (8.76)	**-0.02 (0.08)**†
Larix laricina	125	-7.07 (16.05)	**1.84 (6.16)**†	**0.02 (0.17)**†
Ostrya virginiana	342	**-3.96 (14.15)**†	3.82 (3.56)	0.09 (0.11)
Picea glauca	104	**-1.23 (10.01)**†	**1.15 (8.15)**†	**0.02 (0.12)**†
Picea mariana	160	**-3.68 (20.14)**†	**1.26 (3.73)**†	0.09 (0.14)
Pinus banksiana	95	**-1.80 (7.72)**†	4.33 (3.98)	0.09 (0.15)
Pinus resinosa	206	**-1.32 (6.84)**†	**-2.38 (6.66)**†	-0.07 (0.18)
Pinus strobus	271	**-0.39 (7.67)**†	**-2.40 (11.28)**†	**-0.02 (0.21)**†
Populus grandidentata	141	**-3.16 (13.19)**†	**1.93 (5.40)**†	**0.06 (0.22)**†
Populus tremuloides	595	**-3.23 (18.33)**†	3.09 (4.97)	0.14 (0.20)
Prunus serotina	275	**0.60 (6.29)**†	**0.54 (6.13)**†	0.05 (0.11)
Quercus alba	187	**0.33 (3.83)**†	-9.59 (12.13)	-0.07 (0.13)
Quercus ellipsoidalis	158	**-2.21 (9.53)**†	**-0.75 (9.19)**†	**-0.01 (0.14)**†
Quercus macrocarpa	74	**-0.77 (5.70)**†	**-0.75 (8.52)**†	**0.00 (0.15)**†
Quercus rubra	278	**-1.29 (4.76)**†	**-1.17 (11.10)**†	**-0.04 (0.16)**†
Quercus velutina	85	**0.11 (7.72)**†	**-0.95 (10.81)**†	**0.04 (0.18)**†
Small intolerant hardwood	65	**-0.38 (12.19)**†	-1.26 (2.88)	-0.02 (0.05)
Small tolerant hardwood	37	**1.49 (11.57)**†	1.98 (4.13)	0.05 (0.09)
Thuja occidentalis	165	**-0.57 (11.28)**†	-9.62 (7.02)	-0.22 (0.20)
Tilia americana	326	**0.65 (6.10)**†	-4.18 (9.32)	**-0.02 (0.16)**†
Tsuga canadensis	129	**-0.43 (8.03)**†	-7.39 (10.33)	-0.10 (0.20)
Ulmus americana	269	**-1.39 (8.30)**†	**1.04 (9.60)**†	**0.02 (0.19)**†

Table 4
Calibration for the estimator used to compile basal area m^2/ha. Portions of the growth curves were increased or decreased depending on patterns observed in Figure 4. Results from non-calibrated growth curves for group $A + B$ subplots were compared to the calibrated growth curves for the same $A + B$ group. The abbreviation E corresponds to equivalence at epsilon=0.5.

Scientific name	N	Non-calibrated Mean bias (SD)	Calibrated Mean bias (SD)	Adjustment	Proportional adjustment	TOST total basal area
Abies balsamea	1185	0.0779 (0.1142)	-0.0083 (0.1127)	Decrease growth <12.7cm	0.75	E
Ostrya virginiana	714	-0.1102 (0.1136)	0.0048 (0.0422)	Decrease growth <12.7cm	0.75	E
Picea mariana	313	-0.1071 (0.1492)	-0.0063 (0.1047)	Decrease growth all range	0.55	E
Pinus banksiana	210	-0.1230 (0.1958)	-0.0399 (0.1771)	Decrease growth ≥12.7cm	0.9	E
Populus tremuloides	1204	-0.1676 (0.2290)	0.0083 (0.1591)	Decrease growth all range	0.7	E
Prunus serotina	585	-0.0542 (0.1194)	-0.0077 (0.0827)	Decrease growth <12.7cm	0.55	E
Quercus alba	380	0.0823 (0.1286)	0.0343 (0.1777)	Increase growth all range	3	E
Thuja occidentalis	351	0.2247 (0.2021)	0.0053 (0.1901)	Increase growth all range	0.8	E
Tsuga canadensis	284	0.0970 (0.1729)	0.0721 (0.1910)	Increase growth ≥12.7cm	0.9	E

mean bias in the estimator the lowest among the iterative calibration runs.

3.4. Phase 4: final model validation

From subplot group C, we observed that application of calibrated parameters for the nine corresponding species (Table 4) reduced mean bias in the estimator for basal area (m^2/ha) (Fig. 4 top panel). In addition, despite keeping the parameters for some species unchanged (i.e., non-calibrated), their respective mean bias was affected by competitive interactions with calibrated species (Fig. 4 bottom panel).

We observed that the mean bias associated with the estimator for basal area was reduced for nine species by calibration. Of those nine species, five were ultimately equivalent at an epsilon value of 0.5 (*Ostrya virginiana, Pinus banksiana, Populus tremuloides, Prunus serotina*, and *Thuja occidentalis*) (Table 5).

We observed that calibrating one variable (i.e., basal area) affected model performance for other variables of interest (Table 5). For density, when running a non-calibrated simulation for all species, all of the most abundant species were equivalent. However, when using the calibrated parameters for basal area (Table 4), four out of the 30 were not equivalent. Mean diameter had a direct relationship with basal area calibration since the growth curves (our calibration focus) directly affected mean diameter. When looking at the simulation with non-calibrated parameters, 22 out of the 30 most abundant species were equivalent, compared to the 24 equivalent species when using calibrated parameters.

4. Discussion

Our study presents a novel and replicable framework to evaluate, calibrate, and corroborate a landscape simulation model (LANDIS-II) at

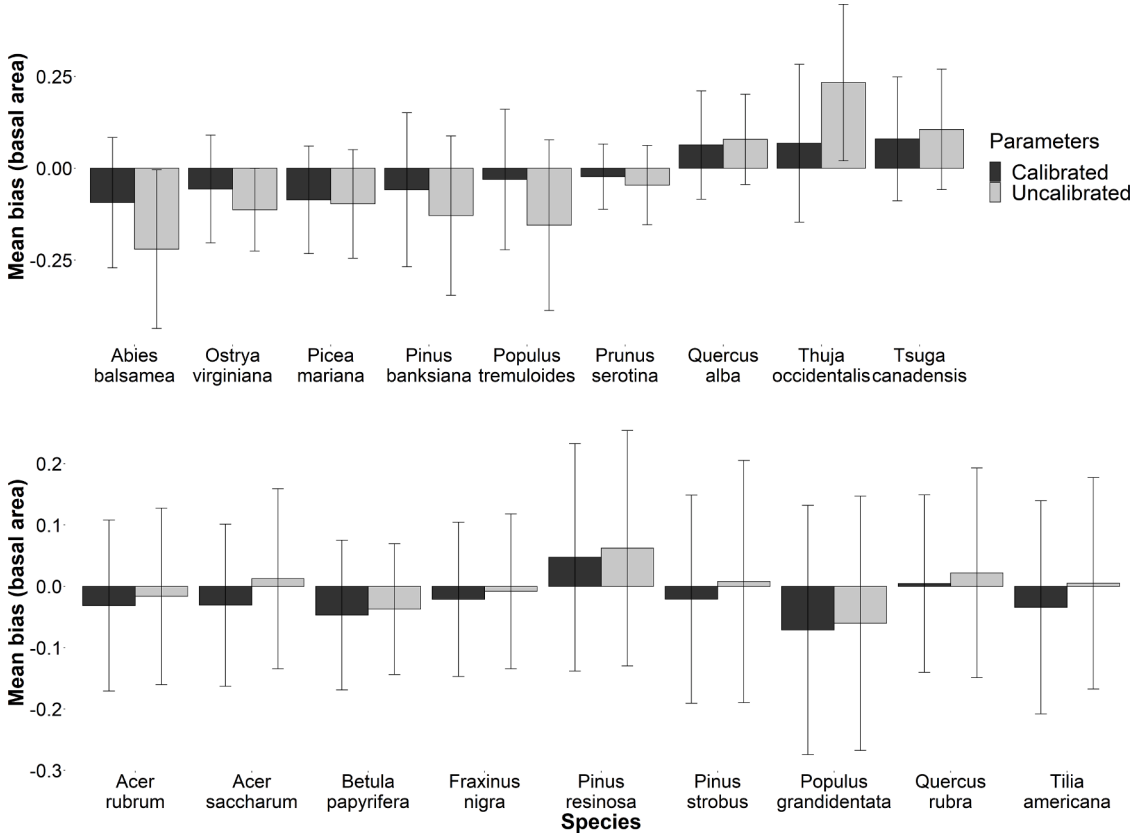

Fig. 4. Mean bias (m^2/ha) in the estimator for basal area from two simulations using calibrated and non-calibrated parameters. The top panel shows the species used for the calibration phase (i.e., calibrated species). The bottom panel shows both simulations for species whose parameters were unchanged (i.e., non-calibrated species).

Table 5
Results from the simulations with group C subplots for density (trees/ha), mean diameter (cm) and basal area (m^2/ha). Cells in bold and with the † symbol represent an equivalent result for the equivalence tests (TOST) with an epsilon of 0.5. Mean bias in the estimator used to obtain predictions is calculated as the difference between observations and predictions. Tree species that underwent calibration are denoted with *.

Scientific name	N	Non-calibrated	Calibrated	Non-calibrated	Calibrated	Non-calibrated	Calibrated
		Basal Area Mean bias (SD)		Density Mean bias (SD)		Mean diameter Mean bias (SD)	
*Abies balsamea**	1144	-0.22 (0.22)	-0.09 (0.18)	**-8.29 (21.4)**†	-12.87 (22.3)	-3.64 (3.92)	**-0.6 (3.5)**†
Acer negundo	160	**-0.05 (0.15)**†	**-0.05 (0.15)**†	**-6.35 (25.16)**†	**-6.28 (25.05)**†	**1.05 (8.39)**†	**0.89 (8.15)**†
Acer rubrum	1964	**-0.02 (0.14)**†	**-0.03 (0.14)**†	**-1.96 (16.71)**†	**-2.07 (16.69)**†	**0.22 (6.46)**†	**-1.07 (4.98)**†
Acer saccharum	1881	**0.01 (0.15)**†	**-0.03 (0.13)**†	**-3.97 (11.41)**†	**-3.78 (11.3)**†	**3.05 (7.62)**†	**0.43 (6.51)**†
Betula alleghaniensis	296	**0.01 (0.09)**†	**0 (0.09)**†	**-0.75 (8.88)**†	**-0.84 (9.29)**†	**2.05 (8.22)**†	**-0.77 (6.4)**†
Betula papyrifera	471	**-0.04 (0.11)**†	**-0.05 (0.12)**†	**-1.48 (11.27)**†	**-1.23 (12.23)**†	**-1.2 (4.41)**†	**-2 (4.78)**†
Carya cordiformis	182	**0 (0.12)**†	**0 (0.13)**†	**-1.38 (8.88)**†	**-1.48 (8.96)**†	**1.01 (7.1)**†	**1.32 (9.17)**†
Carya ovata	171	**0 (0.1)**†	**-0.02 (0.09)**†	**-1.4 (9.12)**†	**-1.22 (8.86)**†	**1.61 (7.77)**†	**-1.86 (6.03)**†
Fraxinus americana	369	**-0.03 (0.13)**†	**-0.04 (0.13)**†	**-4.9 (13.98)**†	**-5.13 (13.96)**†	**0.73 (8.11)**†	**-0.48 (6.76)**†
Fraxinus nigra	673	**-0.01 (0.13)**†	**-0.02 (0.13)**†	**-3.59 (16.69)**†	**-3.49 (16.43)**†	**0.23 (4.82)**†	**-0.78 (4.11)**†
Fraxinus pennsylvanica	252	**-0.03 (0.15)**†	**-0.04 (0.16)**†	**-4.98 (13.75)**†	**-4.92 (14.62)**†	**-0.34 (6.76)**†	**-0.64 (6.84)**†
L_Intolerant conifer	35	-0.06 (0.12)	-0.07 (0.12)	**-2.51 (11.89)**†	-2.6 (12.04)	-3.41 (4.07)	-3.35 (4.17)
L_Intolerant hardwood	23	**-0.02 (0.21)**†	**0.01 (0.25)**†	-4.32 (10.25)	-3.22 (11.63)	**-0.51 (6.26)**†	**-0.44 (5.79)**†
L_Tolerant hardwood	92	**-0.02 (0.09)**†	-0.04 (0.08)	-5.35 (9.92)	-5.28 (9.77)	**2.41 (9.04)**†	**-0.39 (4.48)**†
Larix laricina	249	**-0.01 (0.16)**†	**-0.03 (0.16)**†	**3.28 (18.85)**†	**3.45 (18.86)**†	**-1.21 (6.46)**†	-3.02 (5.38)
*Ostrya virginiana**	658	-0.11 (0.11)	**-0.06 (0.15)**†	**-5.43 (18.02)**†	-11.3 (18.52)	-3.55 (3.83)	**-1.11 (4.47)**†
Picea glauca	203	**-0.05 (0.15)**†	**-0.07 (0.15)**†	**-2.62 (9.43)**†	**-2.93 (9.35)**†	**-1.83 (7.12)**†	**-2.49 (8.08)**†
*Picea mariana**	323	-0.1 (0.15)	**-0.09 (0.15)**†	**-2.79 (19.22)**†	**-6.05 (18.65)**†	-1.63 (3.37)	-2.21 (4.44)
*Pinus banksiana**	198	-0.13 (0.22)	**-0.06 (0.21)**†	**-1.54 (11.98)**†	**-2.68 (11.87)**†	-3.87 (4.94)	**1.23 (5.42)**†
Pinus resinosa	387	**0.06 (0.19)**†	**0.05 (0.19)**†	**0 (8.25)**†	**0.02 (8.1)**†	**2.31 (8.32)**†	**1.08 (6.63)**†
Pinus strobus	530	**0.01 (0.2)**†	**-0.02 (0.17)**†	**-5.08 (18.05)**†	**-5.16 (17.8)**†	**2.51 (11.31)**†	**0 (6.48)**†
Populus grandidentata	343	**-0.06 (0.21)**†	**-0.07 (0.2)**†	**-4.75 (25.41)**†	**-4.51 (25.01)**†	**-2.08 (5.63)**†	**-2.44 (6.58)**†
*Populus tremuloides**	1152	-0.16 (0.23)	**-0.03 (0.19)**†	**-9.85 (36.63)**†	-19.15 (40.52)	-2.64 (5.44)	3.37 (6.38)
*Prunus serotina**	568	**-0.05 (0.11)**†	**-0.02 (0.09)**†	**-4.78 (12.12)**†	-6.24 (13.4)	**-0.14 (5.55)**†	**0.19 (4.84)**†
*Quercus alba**	377	0.08 (0.12)	0.06 (0.15)	**-1.19 (6.94)**†	**0.19 (7.81)**†	10.05 (10.93)	7.48 (12.72)
Quercus ellipsoidalis	291	**-0.02 (0.13)**†	**-0.02 (0.13)**†	**-5.23 (17.89)**†	**-5.3 (18.22)**†	**-0.44 (6.31)**†	**-0.89 (5.38)**†
Quercus macrocarpa	149	**-0.01 (0.16)**†	**-0.02 (0.19)**†	**-1.32 (8.28)**†	**-1.58 (7.89)**†	**0.89 (12.89)**†	**2.09 (16.33)**†
Quercus rubra	537	**0.02 (0.17)**†	**0 (0.14)**†	**-0.61 (8.14)**†	**-0.58 (8.24)**†	**0.42 (9.85)**†	**-1.41 (6.55)**†
Quercus velutina	171	**-0.02 (0.17)**†	-0.06 (0.14)	**-2.15 (9.94)**†	**-2.39 (10.36)**†	**1.29 (12.2)**†	-2.32 (6.09)
S_Intolerant hardwood	164	**0.01 (0.07)**†	**0.01 (0.07)**†	-12.45 (22.79)	-12.79 (22.1)	2.66 (5.34)	2.32 (6.22)
S_Tolerant hardwood	92	-0.04 (0.1)	-0.05 (0.1)	-12.72 (16.28)	-12.95 (16.26)	**-0.41 (4.2)**†	**-0.79 (3.81)**†
*Thuja occidentalis**	352	0.23 (0.21)	**0.07 (0.22)**†	**0.16 (14.3)**†	**3.36 (16.68)**†	9 (6.39)	**-1.16 (5.29)**†
Tilia americana	636	**0.01 (0.17)**†	**-0.03 (0.17)**†	**-2 (11.03)**†	**-1.96 (10.56)**†	**3.06 (9.18)**†	**-1.83 (7.29)**†
*Tsuga canadensis**	274	0.11 (0.16)	0.08 (0.17)	**-0.92 (5.38)**†	**-0.53 (5.72)**†	8.88 (12.1)	5.87 (11.47)
Ulmus americana	585	**-0.03 (0.19)**†	**-0.03 (0.19)**†	**-1.06 (9.71)**†	**-1.11 (9.87)**†	**-1.24 (10.73)**†	**-1.29 (10.83)**†

a site scale using an extensive equal probability sample from the US national forest inventory (i.e., FIA). The design-based unbiased estimators used to obtain empirical estimates from the publicly available FIA data provide a basis for corroboration of a forest landscape model and a consistent source of data for model calibration. The novelty in this study emerges from the scale of observation and the pairwise method of comparison. The traditional approach for landscape models is to examine concurrence, equivalency, or bias in aggregated outputs, where some sources of error may be obscured by variability in multiple processes occurring across the landscape. We performed the iterative calibration and model corroboration using a direct pairwise comparison of simulation outputs and forest inventory data at the plot level. Our approach can be applied by other researchers to enhance model confidence for a wide breadth of questions, such as carbon-fire interactions, effects of disturbances on forest structure and health, and simulation of different forest management scenarios.

Previous corroboration work for landscape simulation models has been conducted for LANDCLIM (Schumacher et al., 2004), iLand (Seidl et al., 2012), and LANDIS PRO (Duan et al., 2021; Huang et al., 2017; C. 2021; Luo et al., 2014; Wang et al., 2014) using experimental or observational data over a short timeframe (two or three decades), similar to that used in this study to corroborate model projections at the species- or site-level scale. Corroboration work for other models like TreeMig (Lischke et al., 2006) and LANDIS-II (McKenzie et al., 2019; Scheller and Mladenoff, 2004) has relied on limited empirical data available for comparison. From these examples, Wang et al. (2014) conducted a corroboration approach most similar to our own in that they applied equivalency tests to the output of a density-based succession model (LANDIS PRO) using a time series of forest inventory data. Their approach differs in two important respects. First, they used a subset of the inventory data that excluded disturbed plots. By using the LU+ extension to implement establishment and disturbance related mortality we were able to assess the processes of growth and competition mortality within the model compared to a wider range of observed data. Second, their evaluations of model predictions for each species were performed at the aggregated ecoregion level, whereas our evaluations were conducted using a pair-wise comparison between individual model cells and FIA subplots.

Such site-level model evaluation is more commonly applied to stand or plot-scale models. For example, Glasby et al. (2019) applied equivalence tests to evaluate diameter growth relationships simulated by the Forest Vegetation Simulator (FVS) model (Crookston and Dixon, 2005; FVS Staff, 2021), with a specific focus on the role of disturbance on residual growth. We demonstrated that similar logic may be applied to landscape models, providing a more rigorous empirical foundation for projections of local processes that can then be scaled to landscapes via their integration with spatially contagious processes such as seed dispersal and disturbances.

Equivalence tests are useful when we expect the differences to be very small and hard to detect. Therefore, the decision of what equivalence threshold to choose is critical. Lakens et al. (2018) proposed several methods for selecting these thresholds based on sample size and effect size of interest. The strength of the equivalence tests relies on the null hypothesis of dissimilarity and examines whether effects extreme enough to be considered meaningful can be rejected (Lakens, 2017). In our case, we used equivalence tests to capture the small differences expected from evaluating a FLM over a short time frame and having most of the model stochastic processes controlled. Since we were using

plot remeasurements, we conducted a pairwise comparison analysis for the equivalence tests where data are not treated as independent (Lakens, 2017). We established a 0.5 threshold for determining equivalency as used in Robinson et al. (2004) and Blanco et al. (2007).

When applying a methodology such as ours to the "evaludation" procedures that develop confidence in a model, the assumptions underlying model design, the representation of processes in the model, scale, and how these factors relate to empirical data are all important factors. In our case, we focused on parameters underlying age-diameter curves as those control how fast a tree grows to determine mean diameter and basal area outputs. We selected our cell size to match a subplot size (i.e., scale). Even so, trees smaller than 12.7 cm dbh within FIA plots are measured from a smaller area (microplot) and assumed to be representative of the entire subplot. Hence discrepancies are anticipated as tree diameters cross the 12.7 cm threshold. We therefore assumed that such discrepancies emerge as statistical noise without bias. Such assumptions would need to be carefully addressed when evaluating model behavior for different resolutions, such as the 0.09 ha or 6.25 ha scales consistent with Landsat and MODIS satellite imagery, respectively. Response variables may also be interdependent. For example, when we calibrated basal area, the density of trees was affected because of the way growing space acts in the model (Table 5). Consequently, fine-tuning equivalence in one variable might result in a loss of equivalence in another variable. Therefore, the primary variable of interest should be chosen in the context of the specific modeling objectives. Finally, the relatively short time span analyzed (20 years) compared to the relatively slow processes of tree growth and mortality may be problematic, so a longer time span of empirical data is clearly desirable.

An important benefit of the iterative approach illustrated by Fig. 2 is that it facilitates better understanding of model process interactions, allowing the model user to learn as they explore complicating factors. This method allows for learning about the model design, application methods and the reference data. For example, the attribute that we were calibrating was species growth rates (age-diameter relationship), which when applied to the generation of initial communities would create slightly different starting cohort diameters. In the initial stage of calibration, we had not accounted for this difference, but the evaluation brought this to our attention, and we integrated this knowledge into the final stage of corroboration. These models are complicated, and it is difficult to anticipate all of the pertinent interactions.

Another learning example resulted in the improvement of a specific model component. Application of the stand density-based mortality model within Density Succession had not been previously tested at this spatial scale and the iterative calibration process highlighted the potential for improving the design of a specific function. Previously the mortality function iterated over cohorts sorted by probability of mortality and removed a proportion of stems within the cohort until the target amount of growing space removed was satisfied. When applying our design to cohorts containing a single tree, we identified a potential source of bias in the species experiencing mortality. This led to a redesign of the looping function to better capture stochasticity within the mortality model.

While equivalence tests represent a formal statistical method for comparison across models, results should still be interpreted with caution. Rejection of a meaningful effect (equivalency) does not imply that an effect is not present at all (Lakens et al., 2018). Therefore, even if our results show equivalency, there might still be some patterns in the data (e.g., environmental gradients, etc.) that represent relevant differences. Furthermore, agreement between modeled and empirical data does not always mean that the model is correct but could also be a factor of an over-calibration or a combination of incorrect representation of processes and input parameters (Augusiak et al., 2014). Therefore, researchers should look at the bigger picture, such as the plausibility of specific parameter ranges, rather than only looking at observed vs predicted values. Over-calibrating parameters can increase the risk of model equivalency for the wrong reasons (i.e., unrealistic parameter combination) (Augusiak et al., 2014). One could guard against such over calibration by approaching the data from different angles, such as equivalency at species versus ecoregion-level (e.g., Fitts Vargas, 2021).

It should be noted that we identified two avenues for calibration: to do it at the ecoregion level or at the species level. For this study we focused on just the species level (See Fitts Vargas, 2021 to explore the ecoregion calibration approach). However, focusing too narrowly on one level can lead to poor behavior elsewhere in the model and should be avoided. In addition, we noticed feedback between parameters when calibrating. Similarly, when the corroboration process improves one variable's behavior, other variables might be affected because of the feedback forest attributes have among each other. Future work could conduct sensitivity analysis to explore additional parameters to calibrate and corroborate.

Our approach may be adapted to address multiple areas of model uncertainty. One might explore the sources of error in this work by grouping plots with other common specific characteristics (i.e., disturbed vs not disturbed) where potentially stronger results may be observed within the small timeframe where data is available. Conducting a sensitivity analysis to explore which model parameters have the most impact during calibration and which contribute the most to confounding other metrics of model performance could be implemented in future work. Other processes within the Density Succession extension of LANDIS-II, such as species cohort recruitment could be evaluated by enabling the regeneration and establishment components of the model. The method is likewise extensible to other geographic regions, other model designs, or both.

5. Conclusions

While FLMs hold very real potential to inform land management and other policy decisions, their adoption for such purposes can be greatly hampered by a lack of confidence in such models (Scheller, 2018; Shifley et al., 2017). This issue is not limited to FLMs, but a concern for environmental modeling generally, with increasing calls for greater transparency, documentation, and rigor in model "evaludation" (Augusiak et al., 2014). Here we present a methodology for evaluating, calibrating, and corroborating LANDIS-II's successional growth algorithms when using its new Density Succession extension at a site scale. This methodology connects empirical data from the US national forest inventory to initialize the landscape, corroborate, and calibrate the model's parameters. This plot/cell evaluation of model behavior is a novel approach compared to the traditional way that evaluation, corroboration, and calibration have been conducted for FLM at landscape levels using summary statistics. These summary statistics might not capture the whole range of variability and bias. The iterative nature of our approach further facilitates learning by the user, where such learning can be thoroughly documented to enhance overall model confidence. The specific succession extension evaluated by our methodology opens a new window of research and development for LANDIS-II users, as Density Succession is directly compatible with common forest inventory measurements and can therefore be integrated with national inventory data in a relatively seamless fashion (as demonstrated here).

There are several sources of potential error to consider when performing such "evaludation" efforts. These sources of bias or error include the corroboration assumptions and study design, the forest inventory sample design, the way certain processes are represented in the model, particular site characteristics, etc. Moreover, calibration can be useful for having the output better match the empirical data, but it should be done with caution. One reason to be cautious is to avoid over calibration (Augusiak et al., 2014). Another reason includes that focusing too narrowly on calibrating at one scale can alter results at another scale (i.e., species vs ecoregions) or for another variable of interest. Therefore, it is important to keep in mind the study's main interest for selecting which variable to calibrate and corroborate.

The cohort characteristics of diameter and density tracked by Density succession are commonly recorded measurements of individual trees in forest inventory datasets. This provides a set of directly comparable metrics for model calibration and corroboration. These cohort characteristics are also frequently used in forest management plans and wildlife habitat models. The emergent processes of stand development based on the stand density index competition process leverages established theories of forest stand dynamics that are unique from other LANDIS-II succession extensions.

The main objective of this paper was to isolate and test specific processes of competition and growth to show how the model is performing. By using individual components (without interactions), we sought to understand the inherent bias (Augusiak et al., 2014). We acknowledge that the interactions between cells are important for the realism of the simulation, however, that would be a next step. Given the caveats above, our approach is extensible to many FLM designs, and should help improve the rigor and transparency of their application.

Funding

This work was supported by the US Department of Agriculture - Forest Service, Northern Research Station (project 14-JV-11242305–012), the Minnesota Agricultural Experiment Station (project MIN-42–101), and University of Minnesota Department of Forest Resources fellowship program.

Code availability

https://github.com/LANDIS-II-Foundation/Extension-Density-Succession/releases/tag/v1.0-beta

https://github.com/jacobf37/Extension-Land-Use-Plus/releases/tag/3.0-beta

https://github.com/LFitts/Landis_Density_Succession

CRediT authorship contribution statement

Lucia A. Fitts: Conceptualization, Data curation, Formal Analysis, Investigation, Methodology, Validation, Visualization, Writing – original draft, Writing – review and editing. **Jacob S. Fraser:** Conceptualization, Methodology, Investigation, Software, Writing – original draft, Writing – review and editing. **Brian R. Miranda:** Conceptualization, Methodology, Investigation, Software, Writing – original draft, Writing – review and editing. **Grant M. Domke:** Conceptualization, Funding Acquisition, Investigation, Resources, Writing – review and editing. **Matthew B. Russell:** Conceptualization, Funding Acquisition, Resources, Project Administration, Supervision, Writing – review and editing. **Brian R. Sturtevant:** Conceptualization, Methodology, Investigation, Writing – review and editing.

Declaration of Competing Interest

The authors declare that they have no known competing financial interests or personal relationships that could have appeared to influence the work reported in this paper.

Data availability

Data used in this research are publicly available in https://apps.fs.usda.gov/fia/datamart/. We have included links to code and software used at the end of our manuscript.

Acknowledgements

We would like to express our gratitude to The USDA Forest Service Northern Research Station and the LANDIS-II Developers group for the constant support on this project, the Forest Inventory and Analysis field crews that collected this data, and to the University of Minnesota Department of Forest Resources. In addition, we would like to thank Eric Gustafson and Hong He for critical reviews of earlier drafts of the manuscript.

Supplementary materials

Supplementary material associated with this article can be found, in the online version, at doi:10.1016/j.ecolmodel.2023.110274.

References

Augusiak, J., Van den Brink, P.J., Grimm, V., 2014. Merging validation and evaluation of ecological models to "evaludation": a review of terminology and a practical approach. Ecol. Modell. 280, 117–128. https://doi.org/10.1016/j.ecolmodel.2013.11.009.

Bagdon, B.A., Nguyen, T.H., Vorster, A., Paustian, K., Field, J.L., 2021. A model evaluation framework applied to the Forest Vegetation Simulator (FVS) in Colorado and Wyoming lodgepole pine forests. For. Ecol. Manage. 480, 118619 https://doi.org/10.1016/j.foreco.2020.118619. October 2020.

Bechtold, W.A., & Patterson, P.L. (2005). The enhanced forest inventory and analysis program-national sampling design and estimation procedures. https://www.srs.fs.usda.gov/pubs/gtr/gtr_srs080/gtr_srs080.pdf.

Blanco, J.A., Seely, B., Welham, C., Kimmins, J.P., Seebacher, T.M., 2007. Testing the performance of a forest ecosystem model (FORECAST) against 29 years of field data in a Pseudotsuga menziesii plantation. Can. J. Forest Res. 37 (10), 1808–1820. https://doi.org/10.1139/X07-041.

Boulanger, Y., Taylor, A.R., Price, D.T., Cyr, D., McGarrigle, E., Rammer, W., Sainte-Marie, G., Beaudoin, A., Guindon, L., Mansuy, N., 2017. Climate change impacts on forest landscapes along the Canadian southern boreal forest transition zone. Landsc. Ecol. 32 (7), 1415–1431. https://doi.org/10.1007/s10980-016-0421-7.

Burns, R., Honkala, B., 1990. Silvics of North America. U.S. Department of Agriculture, Forest Service, p. 877. https://web.archive.org/web/20130214211402/http:/www.na.fs.fed.us/spfo/pubs/silvics_manual/table_of_contents.htm.

Burrill, Ea, Wilson, Am, Turner, Ja, Pugh, Sa, Menlove, Christensen, Conkling, B.L., & David. (2018). FIA database description and user guide for phase 2 (version: 8.0) the forest inventory and analysis database: database description and user guide for phase 2 (version 8.0).

Crookston, N.L., & Dixon, G.E. (2005). The forest vegetation simulator: a review of its structure, content, and applications. Computers and Electronics in Agriculture, 49 (1), 60–80. https://doi.org/10.1016/j.compag.2005.02.003.

Dixon, G. (2002). Essential FVS: a user's guide to the Forest Vegetation Simulator Internal Rep. Fort Collins, CO: U. S. Department of Agriculture, Forest Service, Forest Management Service Center. 226p. (Revised August 2022).

Dixon, G.E., 1986. Prognosis mortality modeling. Internal Report. U.S. Depart. Agricult. Forest Service, Forest Management Service Center, Fort Collins, CO, 10 pp.

Duan, S., He, H.S., Spetich, M.A., Wang, W.J., Fraser, J.S., Thompson, F.R., 2021. Indirect effects mediate direct effects of climate warming on insect disturbance regimes of temperate broadleaf forests in the central U.S. J. Appl. Ecol. 58 (11), 2626–2636. https://doi.org/10.1111/1365-2664.13987.

Fitts, L.A., Domke, G.M., Russell, M.B., 2022. Comparing methods that quantify forest disturbances in the United States' national forest inventory. Environ. Monit. Assess. 194 (4), 1–17. https://doi.org/10.1007/s10661-022-09948-z.

Fitts Vargas, L., 2021. Using the National Forest Inventory to Model and Simulate Forest dynamics, composition, and Land Conversion (Issue November). University of Minnesota.

Franklin, J.F., Mitchell, R.J., Palik, B.J., 2007. Natural disturbance and stand development principles for ecological forestry. Gen. Techn. Rep. 44.

Fraser, J., He, H., Wang, W., 2020. Density-succession v1.0 extension user guide. In: User Guide, p. 36. https://landis-ii-foundation.github.io/Extension-Density-Succession/.

Staff, F.V.S., 2021. Lake States (LS) Variant Overview: Forest Vegetation Simulator (p. 54). USDA Forest Service.

Gao, H., Sabo, J.L., Chen, X., Liu, Z., Yang, Z., Ren, Z., Liu, M., 2018. Landscape heterogeneity and hydrological processes: a review of landscape-based hydrological models. Landsc. Ecol. 33 (9), 1461–1480. https://doi.org/10.1007/s10980-018-0690-4.

Glasby, M.J., Russell, M.B., Domke, G.M., 2019. Analyzing the impacts of forest disturbance on individual tree diameter increment across the US Lake States. Environ. Monit. Assess. 191 (2) https://doi.org/10.1007/s10661-019-7187-8.

Grimm, V., Augusiak, J., Focks, A., Frank, B.M., Gabsi, F., Johnston, A.S.A., Liu, C., Martin, B.T., Meli, M., Radchuk, V., Thorbek, P., Railsback, S.F., 2014. Towards better modelling and decision support: documenting model development, testing, and analysis using TRACE. Ecol. Modell. 280, 129–139. https://doi.org/10.1016/j.ecolmodel.2014.01.018.

Grimm, V., Berger, U., DeAngelis, D.L., Polhill, J.G., Giske, J., Railsback, S.F., 2010. The ODD protocol: a review and first update. Ecol. Modell. 221 (23), 2760–2768. https://doi.org/10.1016/j.ecolmodel.2010.08.019.

He, H.S., 2008. Forest landscape models: definitions, characterization, and classification. For. Ecol. Manage. 254 (3), 484–498. https://doi.org/10.1016/j.foreco.2007.08.022.

Huang, C., He, H.S., Hawbaker, T.J., Liang, Y., Gong, P., Wu, Z., Zhu, Z., 2017. A coupled modeling framework for predicting ecosystem carbon dynamics in boreal forests. Environ. Modell. Softw. 93, 332–343. https://doi.org/10.1016/j.envsoft.2017.03.009.

Huang, C., He, H.S., Liang, Y., Hawbaker, T.J., Henne, P.D., Xu, W., Gong, P., Zhu, Z., 2021. The changes in species composition mediate direct effects of climate change on future fire regimes of boreal forests in northeastern China. J. Appl. Ecol. 58 (6), 1336–1345. https://doi.org/10.1111/1365-2664.13876.

Johnson, R.A., Dixon, G.E., 1986. Adapting models: problems and benefits from incorporating stand density index into the Prognosis Model. Internal Report. U.S. Depart. Agricult. Forest Service, Forest Management Service Center, Fort Collins, CO, 17 pp.

Lakens, Daniel., 2017. Equivalence tests : a practical primer for T tests, correlations, and meta-analyses. Soc. Psychol. Personal Sci. 8 (4), 355–362. https://doi.org/10.1177/1948550617697177.

Lakens, Daniël, Scheel, A.M., Isager, P.M., 2018. Equivalence testing for psychological research: a tutorial. Adv. Methods Pract. Psychol. Sci. 1 (2), 259–269. https://doi.org/10.1177/2515245918770963.

LANDIS II Foundation. (2018). User Guide User Guide. LANDIS II, September, 169–232. www.impact-test.co.uk.

Lischke, H., Zimmermann, N.E., Bolliger, J., Rickebusch, S., Löffler, T.J., 2006. TreeMig: a forest-landscape model for simulating spatio-temporal patterns from stand to landscape scale. Ecol. Modell. 199 (4), 409–420. https://doi.org/10.1016/j.ecolmodel.2005.11.046.

Lucash, M.S., Scheller, R.M., Gustafson, J., Sturtevant B, E.R., 2017. Spatial resilience of forested landscapes under climate change and management. Landsc. Ecol. 32 (5), 953–969. https://doi.org/10.1007/s10980-017-0501-3.

Luo, X., He, H.S., Liang, Y., Wang, W.J., Wu, Z., Fraser, J.S., 2014. Spatial simulation of the effect of fire and harvest on aboveground tree biomass in boreal forests of Northeast China. Landsc. Ecol. 29 (7), 1187–1200. https://doi.org/10.1007/s10980-014-0051-x.

Mayer, A.L., Buma, B., Davis, A.D., GagnCrossed D Sign, S.A., Louise Loudermilk, E., Scheller, R.M., Schmiegelow, F.K.A., Wiersma, Y.F., Franklin, J, 2016. How landscape ecology informs global land-change science and policy. Bioscience 66 (6), 458–469. https://doi.org/10.1093/biosci/biw035.

McKenzie, P., Duveneck, M., Morreale, L., & Thompson, J. (2019). Local and global parameter sensitivity within an ecophysiologically based forest landscape model. Environ. Modell. Softw. https://doi.org/10.1016/j.envsoft.2019.03.002.

McNab, W.H., Cleland, D.T., Freeouf, J.A., Keys, J.E., Jr., Nowacki, G.J., & Carpenter, C. A. (2007). Description of "Ecological subregions: sections of the conterminous United States" (first approximation). 242. https://www.treesearch.fs.fed.us/pubs/48672%0A.

Mladenoff, D.J., He, H.S., 1999. Design, behavior and application of LANDIS, an object oriented model of forest landscape disturbance and succession. Eds.. In: Mladenoff, D.J., Baker, W. (Eds.), Spatial Modeling of Forest Landscape Change: Approaches and applications. Cambridge University Press, pp. 125–162.

Mladenoff, David J. (2004). LANDIS and forest landscape models. In Ecological Modelling (Vol. 180, Issue 1, pp. 7–19). Elsevier. https://doi.org/10.1016/j.ecolmodel.2004.03.016.

Oliver, C., & Larson, B. (1996). Forest Stand Dynamics (1st ed.). ale School of the Environment Other Publications.

Peng, C., 2000. Understanding the role of forest simulation models in sustainable forest management. Environ. Impact Assess. Rev. 20 (4), 481–501. https://doi.org/10.1016/S0195-9255(99)00044-X.

Peterson, G.D., 2002. Contagious disturbance, ecological memory, and the emergence of landscape pattern. Ecosystems 5 (4), 329–338. https://doi.org/10.1007/s10021-001-0077-1.

Reese, G.C., Dymond, C.C., Quigley, K.M., Duveneck, M.J., Lucash, M.S., Gustafson, E.J., Scheller, R.M., Russell, M.B., Miranda, B.R., & Sturtevant, B.R., 2022. Application of growth and yield data and models to calibrate forest landscape models [Manuscript submitted for publication].

Reineke, L.H., 1933. Perfecting a stand-density index for even-aged forests. J. Agric. Res. 46 (7), 627–638.

Robinson, A.P., Froese, R.E., 2004. Model validation using equivalence tests. Ecol. Modell. 176 (3–4), 349–358. https://doi.org/10.1016/j.ecolmodel.2004.01.013.

Scheller, Robert M., Domingo, J.B., Sturtevant, B.R., Williams, J.S., Rudy, A., Gustafson, E.J., Mladenoff, D.J., 2007. Design, development, and application of LANDIS-II, a spatial landscape simulation model with flexible temporal and spatial resolution. Ecol. Modell. 201 (3–4), 409–419. https://doi.org/10.1016/j.ecolmodel.2006.10.009.

Scheller, Robert M., Mladenoff, D.J., 2004. A forest growth and biomass module for a landscape simulation model, LANDIS: design, validation, and application. Ecol. Modell. 180 (1), 211–229. https://doi.org/10.1016/j.ecolmodel.2004.01.022.

Scheller, Robert Michael., 2018. The challenges of forest modeling given climate change. Landsc. Ecol. 33 (9), 1481–1488. https://doi.org/10.1007/s10980-018-0689-x.

Schumacher, S., Bugmann, H., Mladenoff, D., 2004. Improving the formulation of tree growth and succession in a spatially explicit landscape model. Ecol. Modell. 180, 175–194.

Seidl, R., Fernandes, P.M., Fonseca, T.F., Gillet, F., Jönsson, A.M., Merganičová, K., Netherer, S., Arpaci, A., Bontemps, J.-.D., Bugmann, H., González-Olabarria, J.R., Lasch, P., Meredieu, C., Moreira, F., Schelhaas, M.-.J., Mohren, F., 2011. Modelling natural disturbances in forest ecosystems: a review. Ecol. Modell. 222 (4), 903–924. https://doi.org/10.1016/J.ECOLMODEL.2010.09.040.

Seidl, R., Rammer, W., Scheller, R.M., Spies, T.A., 2012. An individual-based process model to simulate landscape-scale forest ecosystem dynamics. Ecol. Modell. 231, 87–100. https://doi.org/10.1016/j.ecolmodel.2012.02.015.

Seidl, R., Thom, D., Kautz, M., Martin-Benito, D., Peltoniemi, M., Vacchiano, G., Wild, J., Ascoli, D., Petr, M., Honkaniemi, J., Lexer, M.J., Trotsiuk, V., Mairota, P., Svoboda, M., Fabrika, M., Nagel, T.A., O Reyer, C.P., 2017. Forest disturbances under climate change. Nature Publishing Group 7. https://doi.org/10.1038/NCLIMATE3303.

Shifley, S.R., He, H.S., Lischke, H., Wang, W.J., Jin, W., Gustafson, E.J., Thompson, J.R., Thompson, F.R., Dijak, W.D., Yang, J., 2017. The past and future of modeling forest dynamics: from growth and yield curves to forest landscape models. Landsc. Ecol. 32 (7), 1307–1325. https://doi.org/10.1007/s10980-017-0540-9.

Stage, A.R., 1973. Prognosis Model For Stand development. Intermountain Forest & Range Experiment Station. US Department of Agriculture, Forest Service.

Stanke, H., Finley, A.O., Domke, G.M., 2022. Simplifying Small area estimation with rFIA: a demonstration of tools and techniques. Front. Forests Global Change 5 (April), 1–13. https://doi.org/10.3389/ffgc.2022.745874.

Stanke, H., Finley, A.O., Weed, A.S., Walters, B.F., Domke, G.M., 2020. rFIA: an R package for estimation of forest attributes with the US Forest Inventory and Analysis database. Environ. Modell. Softw. 127 (February), 104664 https://doi.org/10.1016/j.envsoft.2020.104664.

Sturtevant, B.R., Fortin, M.J., 2021. Understanding and modeling forest disturbance interactions at the landscape level. Front. Ecol. Evol. 9 https://doi.org/10.3389/fevo.2021.653647. October.

Thompson, J., Domingo, J.B., Simons-Legaard, E., Legaard, K., Vyushkov, A., Chmurzynski, A., Laflower, D., & MacLean, M.G. (2021). Land Use Plus (LU+) v3.0 LANDIS-II Extension User Guide.

Thompson, J., Simons-Legaard, E., Legaard, K., Domingo, J.B., 2016. A LANDIS-II extension for incorporating land use and other disturbances. Environ. Modell. Softw. 75, 202–205. https://doi.org/10.1016/j.envsoft.2015.10.021.

Turner, M.G., 2010. Disturbance and landscape dynamics in a changing world. Ecology 91 (10), 2833–2849. https://doi.org/10.1890/10-0097.1.

Vacchiano, G., Motta, R., Bovio, G., Ascoli, D., 2014. Simulator to simulate tree encroachment and Southern Europe. Forest Sci. 60 (April), 241–252.

Verberk, W., 2012. Explaining general patterns in species abundance and distributions. Nature Educ. Knowl. 3 (10), 38.

Wang, W.J., He, H.S., Spetich, M.A., Shifley, S.R., Thompson, F.R., Dijak, W.D., Wang, Q., 2014. A framework for evaluating forest landscape model predictions using empirical data and knowledge. Environ. Modell. Softw. 62, 230–239. https://doi.org/10.1016/j.envsoft.2014.09.003.

Wang, W.J., He, H.S., Spetich, M.A., Shifley, S.R., Thompson, F.R., Larsen, D.R., Fraser, J. S., Yang, J., 2013. A large-scale forest landscape model incorporating multi-scale processes and utilizing forest inventory data. Ecosphere, 4 (9), 1–22. https://doi.org/10.1890/ES13-00040.1.

Woodall, C.W., Miles, P.D., Vissage, J.S., 2005. Determining maximum stand density index in mixed species stands for strategic-scale stocking assessments. For. Ecol. Manage. 216 (1–3), 367–377. https://doi.org/10.1016/j.foreco.2005.05.050.

Zhu, F., Wang, H., Li, M., Diao, J., Shen, W., Zhang, Y., Wu, H., 2020. Characterizing the effects of climate change on short-term post-disturbance forest recovery in southern China from Landsat time-series observations (1988–2016). Front. Earth Sci. 14 (4), 816–827. https://doi.org/10.1007/s11707-020-0820-6.